Nanotechnology **22** (2011) 245609 (7pp) doi:10.1088/0957-4484/22/24/245609

Hierarchical, interface-induced self-assembly of diphenylalanine: formation of peptide nanofibers and microvesicles

Renliang Huang, Rongxin Su, Wei Qi[1], Jun Zhao and Zhimin He

State Key Laboratory of Chemical Engineering, School of Chemical Engineering and Technology, Tianjin University, Tianjin 300072, People's Republic of China

E-mail: qiwei@tju.edu.cn

Received 18 January 2011, in final form 6 April 2011
Published 4 May 2011
Online at stacks.iop.org/Nano/22/245609

Abstract

To gain insight into the hierarchical self-assembly of peptides and the surface effect on assembly formation, an aromatic peptide of diphenylalanine (FF) was used in this study as the model peptide. We found that the diphenylalanine peptide could self-assemble into a core-branched nanostructure through non-covalent interactions in aqueous solution. The pre-assemblies further assembled into nanofibers and microvesicles on the glass surface and microporous membrane, respectively, showing a significant dependence on surface characteristics. The structural and morphological differences between nanofibers and microvesicles were investigated directly using several spectroscopy and microscopy techniques. Our results revealed a hierarchical and interface-induced assembly behavior of diphenylalanine peptide. The novel strategy based on the surface effect allows one to controllably fabricate various peptide-based nanostructures.

S Online supplementary data available from stacks.iop.org/Nano/22/245609/mmedia

(Some figures in this article are in colour only in the electronic version)

1. Introduction

Highly functional and complex structures in biology, created by spontaneous association of molecular units, have motivated our great interest in self-assembly of synthetic systems [1–3]. A wide variety of artificial self-assembling systems have been developed, such as peptides, proteins, carbohydrates, nucleic acids and their derivatives [4–9]. In this respect, the self-assembled peptide nanostructures have been the focus of considerable research in recent years. A number of peptide-based building blocks, including hydrophobic dipeptides [10–14], surfactant-like peptides [15], amyloid peptide fragments [16, 17], peptide-amphiphile [18] and cyclic peptides [19], have been designed and developed for the construction of organized supramolecular nanostructures. Due to their good biocompatibility and extensive functional diversity, nanomaterials are extremely attractive for various applications [2, 18]. Despite the increasing scientific knowledge about the peptide-based architectures and their potential applications, the assembly mechanism of peptides is still unclear in many cases, especially the process of hierarchical self-assembly [20], which is initiated by the assembly of molecular-scale building units into clusters and then further organized to form more complicated assembling structures, like nanotubes, nanofibers and nanovesicles.

There exists many hierarchical self-assembly processes leading to the functional structures in biology as well as in synthetic systems, which involve the molecule–molecule, molecule–solvent and molecule–substrate interactions [20]. A large part of this research is towards the interactions of molecules and the effects of solution conditions such as solvent, temperature, pH and ionic strength. However, many aspects of the molecule–substrate interactions still remain obscure due to the difficulties in nanoscale *in situ* examination

[1] Author to whom any correspondence should be addressed.

of the assemblies. The results obtained by SEM and TEM techniques do not always exhibit the real morphologies of peptide assemblies in solution, because the samples are commonly dried on the substrate before detection. Recent reports have shown that the surface plays an important role in the formation of peptide assemblies, for instance, amyloid-β (Aβ) peptide and EAK16-II [21, 22], which indicates that the surface effect on peptide self-assembly is critical to the nanostructure formation. Multilevel molecular self-assembly on surfaces/interfaces have been applied to the construction of ordered nanostructures, but it is a challenge to profoundly understand the principles and accurately control the growth of higher level assemblies from elemental building blocks [20].

Gazit and co-workers have developed the self-assembling diphenylalanine (FF) system that created functional peptide nanotubes [11, 23]. Subsequently, some studies reported that diphenylalanine could be organized into nanowires/nanofibers and microcrystals according to its growth conditions [24–26]. In the self-assembling diphenylalanine system, the incorporation of non-covalent interactions, including hydrogen bonds, π–π stacking, steric interactions and hydrophobic forces, render the assembly process extremely complex. So far, there is still a notable lack of understanding how to construct diphenylalanine assemblies with morphological diversity. The effect of surfaces/interfaces (solution–solid or gas–solid) on nanostructures growth has also not been studied sufficiently. In this study, we investigated the hierarchical self-assembly behaviors of diphenylalanine peptide, as well as the surface effect on assembly formation.

2. Experimental methods

2.1. Materials

The lyophilized diphenylalanine (NH_2–Phe-Phe–COOH, FF) peptide was purchased from Bachem (Bubendorf, Switzerland). 1,1,1,3,3,3-hexafluoro-2-propanol (HFIP) was purchased from Sigma-Aldrich. Microscopic glass coverslips and microporous mixed cellulose ester membranes (cellulose nitrate/cellulose acetate = 4; pore size 0.22 μm) were obtained from commercial sources.

2.2. Preparation of peptide nanofibers and microvesicles

The diphenylalanine stock solution was freshly prepared by dissolving the peptides in HFIP at a concentration of 100 mg ml^{-1} (prepared just before use). The FF peptide stock solution was then diluted to a final concentration of 0.02, 0.2, 0.5 and 2 mg ml^{-1} in ddH_2O, respectively. The resulting solutions were shaken for several seconds, and then aged at room temperature for one day without disturbance.

A 30 μl aliquot of FF solutions with different concentrations were dripped onto microscopic glass coverslips and microporous membranes. After overnight drying at ambient temperature, peptide assemblies were formed and then observed by scanning electron microscopy (SEM).

To observe the real morphology of peptide assemblies in solution, a 5 μl drop of 0.5 mg ml^{-1} FF solution was placed on a freshly cleaved mica surface and then covered carefully with an another freshly cleaved mica. The resulting thin layer of FF solution together with the mica slip was frozen quickly by immersion in liquid nitrogen for 2 min. Subsequently, the frozen FF solution was dried by a freeze drier (Christ Alpha1-2, Osterode, Germany) under vacuum conditions (0.33 mbar).

2.3. Morphology characterization

2.3.1. Scanning electron microscopy. All the samples were sputter-coated with platinum using an E1045 Pt-coater (Hitachi High-technologies Co., Japan), and then imaged by a S-4800 field emission scanning electron microscope (Hitachi High-technologies Co., Japan) at the acceleration voltage of 5 kV.

2.3.2. Transmission electron microscopy. A 10 μl aliquot of FF solution (2 mg ml^{-1}) was placed onto a carbon-coated copper grid, air-dried for approximately one hour, and then examined in a JEOL 100CX-II (80 kV, JEOL Ltd, Japan) without staining.

2.3.3. Atomic force microscope. The samples for atomic force microscope (AFM) measurement were prepared according to the method of quick-freeze/vacuum drying. The AFM images were obtained by using a CSPM 5000 (Ben Yuan Ltd, China) in tapping mode.

2.3.4. Laser scanning confocal microscope. A 100 μl aliquot of 2 mg ml^{-1} FF solution (aged for one day) was diluted to a final concentration of 0.5 mg ml^{-1} with ddH_2O. A 30 μl aliquot of FF solution (2 mg ml^{-1} without dilution or 0.5 mg ml^{-1} after dilution) was placed on a slide glass and then covered with a cover glass. The samples were scanned immediately on a laser scanning confocal microscope (FV1000, Olympus, Japan). A laser at 370 nm was used to excite the FF molecules.

2.4. Size distribution measurement

The size distribution and volume-weighted mean diameter (d) of FF assemblies in solution were determined by using a Zetasizer Nano (0.6 nm–6 μm, Malvern Instruments, UK) and a Mastersizer S (4–3500 μm, Malvern Instruments, UK) particle size analyzer, respectively.

2.5. CD spectroscopy

Circular dichroism (CD) spectra of FF solutions were measured on a JASCO J-810 CD spectropolarimeter at room temperature over a wavelength range of 185–260 nm. A quartz cell with 10 mm, 1 mm, 0.1 mm and 0.1 mm path length were used for CD measurements of 0.02, 0.2, 0.5 and 2 mg ml^{-1} FF solutions, respectively.

2.6. Fourier transform infrared spectroscopy

The aged FF solution (2 mg ml^{-1}) was air-dried on a KBr plate and then transferred to a desiccator before measurement. The FTIR spectra of FF assemblies were recorded on a Nicolet-560E.S.P FTIR spectrometer with 20 scans and a resolution of 4 cm^{-1}.

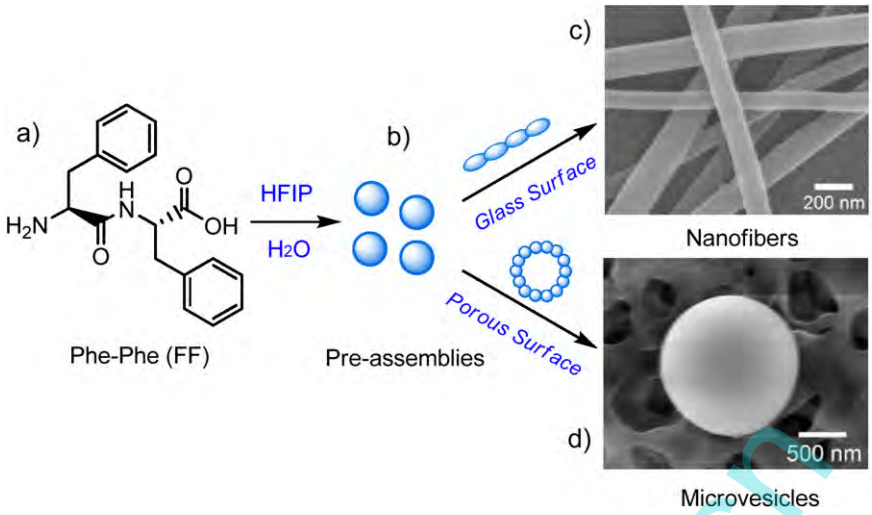

Scheme 1. Proposed hierarchical self-assembly mechanism for the formation of peptide assemblies. (a) The constitutional formula of diphenylalanine peptide (FF); (b) self-assembly of FF into pre-assemblies in aqueous solution; (c) an SEM image of nanofibers formed on the glass surface (0.5 mg ml^{-1}) and (d) an SEM image of microvesicles formed on the surface of microporous cellulose ester (0.5 mg ml^{-1}).

3. Results and discussion

The proposed hierarchical assembly mechanism of diphenylalanine is illustrated in scheme 1. In a typical experiment, the lyophilized diphenylalanine was dissolved in HFIP and then diluted into aqueous solution at a final concentration of 0.5 mg ml^{-1}. The resulting solution was shaken for several seconds, forming a transparent solution. Then aliquots of FF solutions were dripped onto glass coverslips and microporous cellulose ester membranes. After overnight drying at ambient temperature, peptide nanofibers and microvesicles were formed and deposited on the surfaces of glass coverslips and microporous membranes, respectively. On the basis of our findings, we assume that the formation of nanofibers and microvesicles is an interface-induced assembly process where surface characteristics play an important role in the construction of different FF assemblies.

We used scanning electron microscopy (SEM) to study the morphologies of FF nanofibers and microvesicles formed on the different surfaces. The solid-cored FF nanofibers with different end shapes were observed on the glass surface in our study (figures 1(a), (b) and S1 available at stacks.iop.org/Nano/22/245609/mmedia). SEM images showed that the FF nanofibers were 50 nm to 1 μm in diameter and at least 100 μm in length. The structure of nanofibers was significantly different from the results by Han [25] and Ryu [24] in which short nanowires were formed under different conditions. Han *et al* [25] proposed that the interface–solvent interaction between the assembled structure and surrounding nonpolar CS_2 results in nanowire morphology. Another study by Ryu *et al* [24] reported that the amine group in aniline, which can act as a hydrogen-bond donor, may influence the formation of hydrogen bonds and thus lead to the formation of crystalline FF nanowires. In this study, FF was assembled in water and then deposited on glass surface, leading to the formation of FF nanofibers. The formation of peptide nanofibers occurred when the initial concentration of FF was higher than 0.5 mg ml^{-1}. If the FF concentration decreased to 0.2 mg ml^{-1}, random aggregate structures were observed (figure S1(d) available at stacks.iop.org/Nano/22/245609/mmedia). Transmission electron microscopy (TEM) was also used to characterize the FF assemblies (figure 2). The TEM results (without staining) further confirmed the fibrillar structure formed on the surface of a carbon-coated copper grid.

Interestingly, when the aged FF solutions were dripped onto microporous membranes and subsequently air-dried, microvesicles with diameters ranging from 1–3 μm were obtained on the film surface (figures 1(c), (d) and S2 available at stacks.iop.org/Nano/22/245609/mmedia). Likewise, the morphology of FF microvesicles found in our study was remarkably different from that reported previously, such as nanotubes, nanowires/nanofibers and microcrystal structures formed under different solvent conditions [11, 24–26]. Our results revealed a new pathway for diphenylalanine self-assembly that led to the formation of organized FF microvesicles. At different FF concentrations (0.02–2 mg ml^{-1}), microvesicles could be observed on the surface of microporous cellulose ester membranes. In particular, macrofibers were also found on the surface when the FF concentration reached 2 mg ml^{-1} (figure S2(a) available at stacks.iop.org/Nano/22/245609/mmedia). To determine whether the macrofibers were formed on the surface or in aqueous solution, SEM and laser scanning confocal microscopy (LSCM) was employed for imaging the morphology of FF aggregates in high concentration solution (figure S3 available at stacks.iop.org/Nano/22/245609/mmedia). The results showed that the macrofibers were formed via FF self-assembly in aqueous solution with high concentration, which were consistent with the experimental phenomena that visual formation of assemblies occurred at 2 mg ml^{-1} FF concentration within several seconds. According to our results, we proposed that a part of FF monomers were aggregated to macrofibers when the

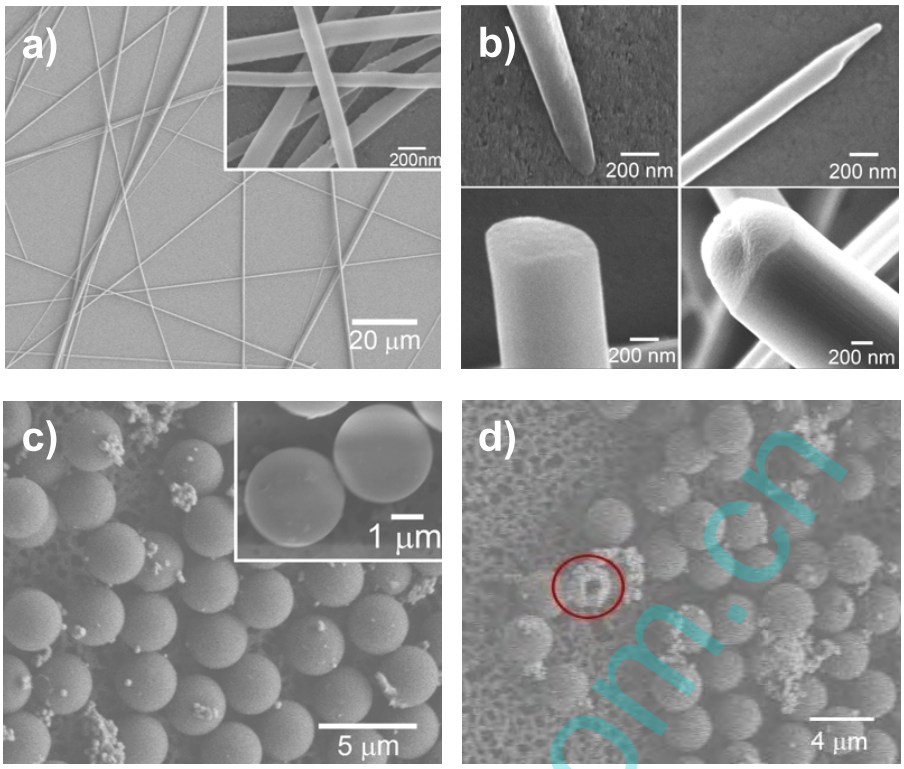

Figure 1. SEM micrographs of FF assemblies formed on the surfaces of glass coverslips ((a), (b)) and microporous cellulose ester membranes ((c), (d)). The solid-cored FF nanofibers (b) and the hollow microvesicles (d) were found in the SEM images. The peptide nanofibers and microvesicles were formed at the starting concentrations of 0.5 mg ml^{-1} and 0.2 mg ml^{-1}, respectively.

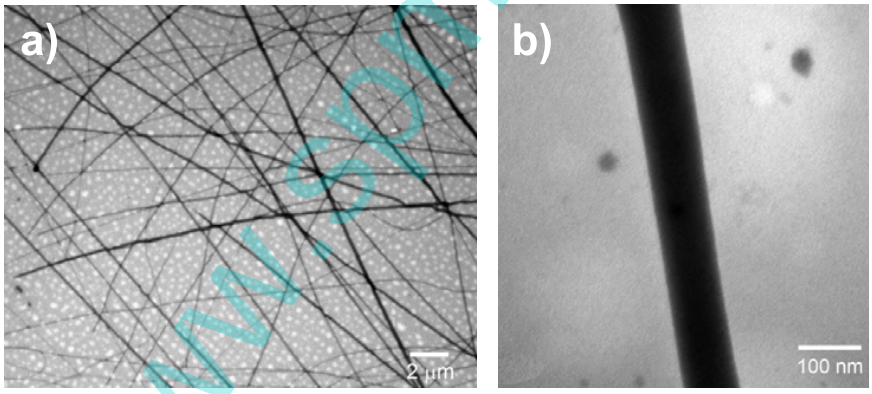

Figure 2. TEM micrographs of FF nanofibers formed on the surface of a carbon-coated copper grid at the starting concentration of 2 mg ml^{-1}.

FF concentration reached a critical value, while the residual molecules were assembled into intermediate nanostructures (pre-assemblies) in aqueous solution and further organized into nanofibers or microvesicles on different surfaces.

To obtain the real morphology of pre-assemblies in aqueous solution, the samples were prepared by quick freezing with liquid nitrogen and then drying under vacuum. Surprisingly, we observed the core-branched structure of pre-assemblies in both SEM and AFM images (figures 3(a), (b), and S4 available at stacks.iop.org/Nano/22/245609/mmedia). The similar structures were also found in other self-assembly systems such as guanosine [27]. However, the formation mechanism of branched nanostructures is still unclear. When an aliquot of FF solution was placed on a glass surface, frozen at −40 °C and then dried under vacuum, the intermediate states in FF peptide assembly from pre-assemblies to nanofibers can be observed directly (figures 3(c) and (d)). The images showed that the size of the central core was approximately 100 nm–1 μm and the average length of the branches linked to the core was about 1 μm. A laser diffraction size analyzer was employed to further determine the size distribution of FF pre-assemblies at different concentrations (figure 4(a)), showing that the FF pre-assemblies had a relative broad size distribution, which resulted in the formation of nanofibers

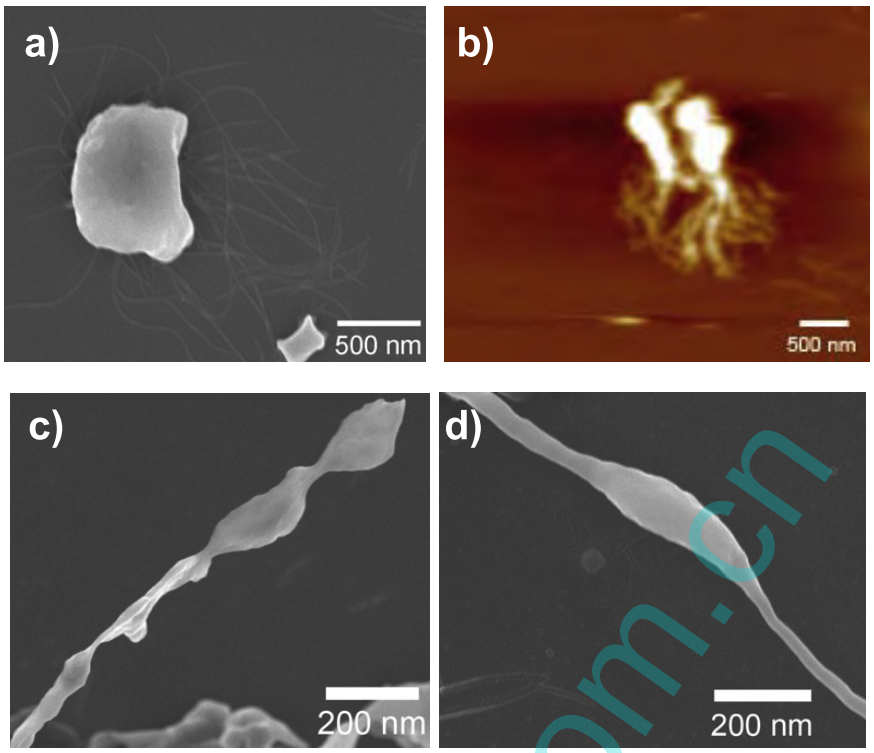

Figure 3. Microscopic analysis of FF pre-assemblies in solution. (a) SEM image and (b) AFM image of the dried pre-assemblies (0.5 mg ml^{-1}) prepared by using a quick-freeze/vacuum drying method and ((c), (d)) SEM images of the FF assemblies on the glass surface; the samples were frozen at −40 °C and then dried under vacuum.

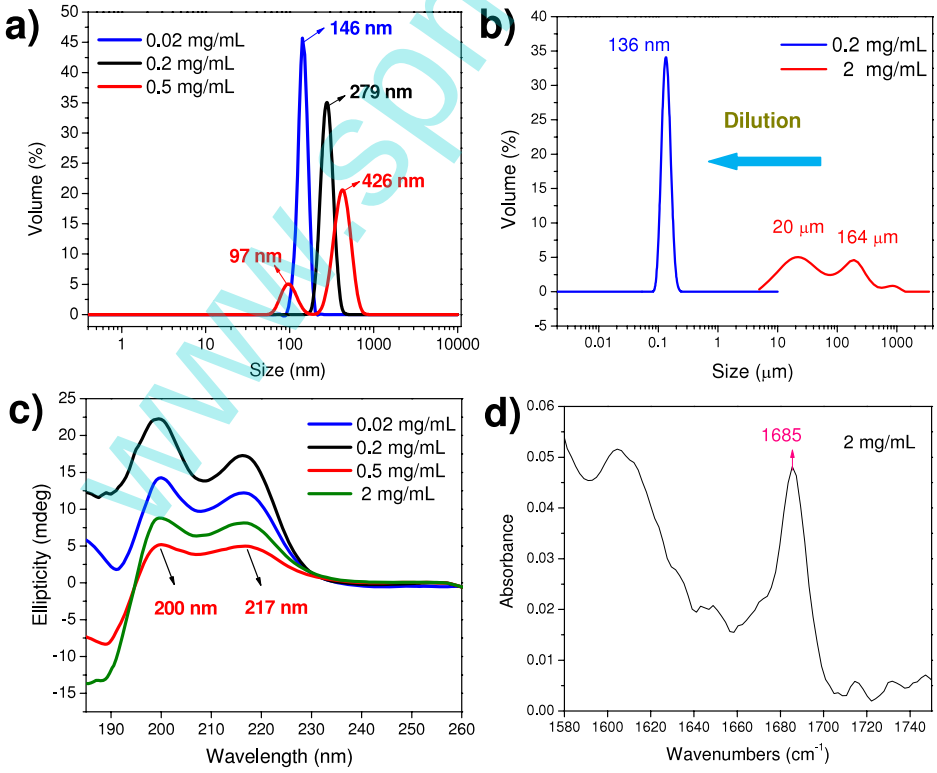

Figure 4. (a) Size distribution of FF pre-assemblies in solution; (b) change in size distribution of FF assemblies during the dilution process (2 mg ml^{-1} FF solution was diluted to a final concentration of 0.2 mg ml^{-1} with ddH_2O); (c) CD spectra of FF pre-assemblies in solution. Quartz cells with 10 mm, 1 mm, 0.1 mm and 0.1 mm path length were used for CD measurements of 0.02, 0.2, 0.5 and 2 mg ml^{-1} FF solution, respectively, and (d) FTIR spectrum (amide I region) of the FF assemblies.

or microvesicles with a wide range of size distributions. In addition, we found that the macrofibers formed at 2 mg ml^{-1} could be disaggregated into pre-assemblies under dilution in aqueous solution (figure 4(b)).

The secondary structures of FF peptides in self-assembly process were investigated by using circular dichroism (CD) and Fourier transform infrared spectra (FTIR). The CD spectra of FF pre-assemblies in aqueous solution showed a negative peak at 190 nm, and two positive peaks at 200 nm and 217 nm corresponding to the π–π^* transition and n–π^* transition, respectively [28] (figure 4(c)). The shape of the CD curves was similar to that of β-turn peptides, which was characterized by a negative peak at 180–190 nm and two positive peaks at 200–205 nm and 220–230 nm [29]. When the FF nanofibers formed on the glass surface were dispersed in the aqueous solution, the CD results showed that the secondary structure of nanofibers remained unchanged (figure S5 available at stacks.iop.org/Nano/22/245609/mmedia). The FTIR spectrum showed a sharp amide I absorption band at 1685 cm^{-1} (figure 4(d)), which was also contributed by the turns' secondary structure [28, 30]. Therefore, CD and FTIR results altogether indicated that the FF monomers may be stacked in a β-turn arrangement with hydrogen bonding between the peptides.

Although we lack a clear picture of how the diphenylalanine peptide assembled into pre-assemblies in aqueous solution and further organized into nanofibers or microvesicles on different surfaces, we can analyze the key factor determining the morphologies of peptide assemblies and gain some insights into how to govern the assembly process. In the FF self-assembly system, liquid crystalline nanowires and organogels can be obtained in CS_2 and toluene solvents, respectively [25, 28], indicating that solvent plays an important role in directing FF self-assembly into supramolecular structures. Recently, Heredia *et al* [31] reported a temperature-driven phase transformation in self-assembled FF nanotubes, in which the inter-tube condensation energy is determined at the level of E_{con} = 2.5–4.4 kcal mol^{-1} and as a result it could be easily rearranged from one to another polymorphic transformation along with the temperature increase, occurring due to a very wide variation of peptide bond torsion angle [31, 32]. Except for the solvent and temperature-dependent structural transition, in this study, interface–surface interactions could also result in the different structure of FF assemblies under differences of interactions between FF and substrates. In the process of nanofiber or microvesicle formation, surface characteristics, including surface tension (or surface energy), hydrophilicity/hydrophobicity, porosity or roughness, are a key factor that has direct impact on the morphologies of FF assemblies. We used another four substrates, Si, regenerated cellulose, polyethersulfone and porous alumina, to examine the influence of surface characteristics on FF self-assembly. The SEM images of FF assemblies were shown in figure S6 (available at stacks.iop.org/Nano/22/245609/mmedia). It can be seen that FF nanofibers can also been formed on the surface of Si and regenerated cellulose, while random aggregation and flake structure formed on polyethersulfone and porous alumina, respectively. Among these flat substrates (glass, Si, cellulose and polyethersulfone), polyethersulfone has the highest surface tension (50 dynes cm^{-1} [33]). Therefore, low surface tension could help the self-assembly of FF pre-assemblies into nanofibers, while high surface tension may lead to their random aggregation. The role of surface tension on molecular self-assembly had also been demonstrated in many previous studies [34, 35]. However, the relationship between surface tension and FF assembly is not actually settled and needs further studies and confirmation. In addition, the different FF assemblies formed on the microporous cellulose and alumina membranes suggested that porosity alone is not the dominant role in the formation of microvesicles. Multi-interactions between FF peptide and substrates with various surface characteristics render the assembly process extremely complex, and further detailed study is still needed to better understand the mechanisms involved in this process.

4. Conclusions

In this study, we demonstrated a hierarchical assembly of diphenylalanine peptide which formed nanofibers and microvesicles on different surfaces from the pre-assemblies organized via non-covalent interactions in aqueous solution. The morphological difference between nanofibers and microvesicles was closely related to the surface characteristics. The real morphology of pre-assemblies in solution was firstly observed as core-branched nanostructures using a quick-freeze/vacuum drying method. Furthermore, we studied the secondary structure of FF pre-assemblies and nanofibrils by CD and FTIR spectroscopies, indicating the hydrogen bonding interaction between the peptide FF monomers which may be stacked in β-turn arrangement. In summary, our results revealed a hierarchical and interface-induced assembly behavior of FF, which allowed us to fabricate nanofibers and microvesicles based on the different surface characteristics, and thus a novel strategy concerning the surface effect was proposed for the peptide-based nanofabrication.

Acknowledgments

This work was supported by the Program for New Century Excellent Talents in Chinese University (NCET-08-0386), the Key Project of Chinese Ministry of Education (108031), the 863 Program of China (2008AA10Z318), the Natural Science Foundation of China (20976125, 20806057 and 31071509) and Tianjin (10JCYBJC05100), and the Program of Introducing Talents of Discipline to Universities of China (B06006).

References

[1] Fan T X, Chow S K and Di Z 2009 Biomorphic mineralization: from biology to materials *Prog. Mater. Sci.* **54** 542–659
[2] Gao X Y and Matsui H 2005 Peptide-based nanotubes and their applications in bionanotechnology *Adv. Mater.* **17** 2037–50
[3] Hartgerink J D, Beniash E and Stupp S I 2002 Peptide-amphiphile nanofibers: a versatile scaffold for the preparation of self-assembling materials *Proc. Natl Acad. Sci. USA* **99** 5133–8
[4] Scanlon S and Aggeli A 2008 Self-assembling peptide nanotubes *Nano Today* **3** 22–30

[5] Graveland-Bikker J F, Schaap I A T, Schmidt C F and de Kruif C G 2006 Structural and mechanical study of a self-assembling protein nanotube *Nano Lett.* **6** 616–21
[6] Gattuso G, Menzer S, Nepogodiev S A, Stoddart J F and Williams D J 1997 Carbohydrate nanotubes *Angew. Chem. Int. Edn* **36** 1451–4
[7] Rothemund P W K, Ekani-Nkodo A, Papadakis N, Kumar A, Fygenson D K and Winfree E 2004 Design and characterization of programmable DNA nanotubes *J. Am. Chem. Soc.* **126** 16344–52
[8] Palmer L C, Newcomb C J, Kaltz S R, Spoerke E D and Stupp S I 2008 Biomimetic systems for hydroxyapatite mineralization inspired by bone and enamel *Chem. Rev.* **108** 4754–83
[9] Matsui H and Gologan B 2000 Crystalline glycylglycine bolaamphiphile tubules and their pH-sensitive structural transformation *J. Phys. Chem.* B **104** 3383–6
[10] Gorbitz C H 2007 Microporous organic materials from hydrophobic dipeptides *Chem.—Eur. J.* **13** 1022–31
[11] Reches M and Gazit E 2003 Casting metal nanowires within discrete self-assembled peptide nanotubes *Science* **300** 625–7
[12] Zhou M, Smith A M, Das A K, Hodson N W, Collins R F, Ulijn R V and Gough J E 2009 Self-assembled peptide-based hydrogels as scaffolds for anchorage-dependent cells *Biomaterials* **30** 2523–30
[13] Yan X H, Zhu P L and Li J B 2010 Self-assembly and application of diphenylalanine-based nanostructures *Chem. Soc. Rev.* **39** 1877–90
[14] Yan X H, Cui Y, Qi W, Su Y, Yang Y, He Q and Li J B 2008 Self-assembly of peptide-based colloids containing lipophilic nanocrystals *Small* **4** 1687–93
[15] Yang Y L, Khoe U, Wang X M, Horii A, Yokoi H and Zhang S G 2009 Designer self-assembling peptide nanomaterials *Nano Today* **4** 193–210
[16] Lu K, Jacob J, Thiyagarajan P, Conticello V P and Lynn D G 2003 Exploiting amyloid fibril lamination for nanotube self-assembly *J. Am. Chem. Soc.* **125** 6391–3
[17] Krysmann M, Castelletto V and Hamley I 2007 Fibrillisation of hydrophobically modified amyloid peptide fragments in an organic solvent *Soft Matter* **3** 1401–6
[18] Cui H G, Webber M J and Stupp S I 2010 Self-assembly of peptide amphiphiles: from molecules to nanostructures to biomaterials *Biopolymers* **94** 1–18
[19] Bong D T, Clark T D, Granja J R and Ghadiri M R 2001 Self-assembling organic nanotubes *Angew. Chem. Int. Edn* **40** 988–1011
[20] Yang Y L and Wang C 2009 Hierarchical construction of self-assembled low-dimensional molecular architectures observed by using scanning tunneling microscopy *Chem. Soc. Rev.* **38** 2576–89
[21] Kowalewski T and Holtzman D M 1999 *In situ* atomic force microscopy study of Alzheimer's beta-amyloid peptide on different substrates: new insights into mechanism of beta-sheet formation *Proc. Natl Acad. Sci. USA* **96** 3688–93
[22] Yang H, Fung S Y, Pritzker M and Chen P 2007 Surface-assisted assembly of an ionic-complementary peptide: controllable growth of nanofibers *J. Am. Chem. Soc.* **129** 12200–10
[23] Adler-Abramovich L, Badihi-Mossberg M, Gazit E and Rishpon J 2010 Characterization of peptide-nanostructure-modified electrodes and their application for ultrasensitive environmental monitoring *Small* **6** 825–31
[24] Ryu J and Park C B 2008 High-temperature self-assembly of peptides into vertically well-aligned nanowires by aniline vapor *Adv. Mater.* **20** 3754–8
[25] Han T H, Kim J, Park J S, Park C B, Ihee H and Kim S O 2007 Liquid crystalline peptide nanowires *Adv. Mater.* **19** 3924–7
[26] Zhu P L, Yan X H, Su Y, Yang Y and Li J B 2010 Solvent-induced structural transition of self-assembled dipeptide: from organogels to microcrystals *Chem.—Eur. J.* **16** 3176–83
[27] Li Y L, Dong M D, Otzen D E, Yao Y H, Liu B, Besenbacher F and Mamdouh W 2009 Influence of tunable external stimuli on the self-assembly of guanosine supramolecular nanostructures studied by atomic force microscope *Langmuir* **25** 13432–7
[28] Yan X H, Cui Y, He Q, Wang K W and Li J B 2008 Organogels based on self-assembly of diphenylalanine peptide and their application to immobilize quantum dots *Chem. Mater.* **20** 1522–6
[29] Rodger A and Nordén B 1997 *Circular Dichroism and Linear Dichroism* (New York: Oxford University Press)
[30] Gupta M, Bagaria A, Mishra A, Mathur P, Basu A, Ramakumar S and Chauhan V S 2007 Self-assembly of a dipeptide-containing conformationally restricted dehydrophenylalanine residue to form ordered nanotubes *Adv. Mater.* **19** 858–61
[31] Heredia A, Bdikin I, Kopyl S, Mishina E, Semin S, Sigov A, German K, Bystrov V, Gracio J and Kholkin A L 2010 Temperature-driven phase transformation in self-assembled diphenylalanine peptide nanotubes *J. Phys. D: Appl. Phys.* **43** 462001
[32] Gorbitz C H 2001 Nanotube formation by hydrophobic dipeptides *Chem.—Eur. J.* **7** 5153–9
[33] TAPPI 2007 Determination of wetting tension of polymeric films and coated surfaces via the Mayer rod technique www.tappi.org
[34] Syms R R A, Yeatman E M, Bright V M and Whitesides G M 2003 Surface tension-powered self-assembly of micro structures—the state-of-the-art *J. Microelectromech. Syst.* **12** 387–417
[35] Sun B Q and Sirringhaus H 2006 Surface tension and fluid flow driven self-assembly of ordered ZnO nanorod films for high-performance field effect transistors *J. Am. Chem. Soc.* **128** 16231–7